Hindawi
Advances in Civil Engineering
Volume 2018, Article ID 9787429, 10 pages
https://doi.org/10.1155/2018/9787429

Research Article

Constitutive Model and Damage Evolution of Mudstone under the Action of Dry-Wet Cycles

Ming Hu,[1] **Yuanxue Liu**,[1] **Linbo Song**,[1] **and Yu Zhang**[2]

[1]*Chongqing Key Laboratory of Geomechanics and Geoenvironment Protection, Army Logistics University of PLA, Chongqing 401311, China*
[2]*Naval Logistics Academy, Tianjin 300450, China*

Correspondence should be addressed to Yuanxue Liu; 357202780@qq.com

Received 22 December 2017; Accepted 21 March 2018; Published 2 May 2018

Academic Editor: Yixian Wang

Mudstone is a natural type of geological material, which has different ways of mechanical response between natural state and dry-wet cycles. According to the complex damage theory of geological materials, rock masses can be considered as a composite material consisting of the structure phase and damage phase. The essence of the damage of rock masses is a damage evolution process, during which the deformation energy of the structure phase converts into dissipation energy of the damage phase, and the energy dissipation from phase transformation promotes the structure phase to change into the damage phase. In this study, a customized model test container and a novel test method are applied to study the decay rate of mudstone under different temperatures and over multiple dry-wet cycles. The decay rate and the damage variable are connected with each other and applied to the damage constitutive equation based on the energy principle to set up the damage evolution equation under the coupled action of dry-wet cycles and loads. Comparison of the proposed model with test results in a literature identifies the rationality of the established model and properly reflects the damage evolution of mudstone.

1. Introduction

Mudstone is a natural type of geological material. Its mechanical responses vary under the action of natural state and dry-wet cycles [1]. After multiple dry-wet cycles, mudstone is easy to weather and disintegrate. For example, the water level variation of reservoir bank for a long time and the underground water variation caused by rainfall and pumping may lead to slope failure or ground subsidence. Therefore, researches on the physical and mechanical characteristics of mudstone under the action of dry-wet cycles increase gradually. Cantón et al. [2] found that the number of dry-wet cycles had the strongest influence on weathering. Guo et al. [3] studied the effect of alternation of heat and water on the slaking phenomenon of redbeds and concluded that the disintegration of mudstone was the result of the comprehensive action of wetting, heating, and loading. Qi et al. [4] concluded that the main mechanisms of slaking of red strata mudstone were water absorption, dehydration shrinkage during drying, and mineral dissolution. Even so, currently there are few researches about the damage of mudstone under the action of dry-wet cycles and the damage constitutive model under the coupled action of dry-wet cycles and loads.

Damage evolution of rock is an important issue in the study of rock mass damage mechanics [5–9]. The rock material is anisotropic, in which there are microcracks and macroscopic defects such as cracks, bubbles, cavities, and joints. Crack propagation makes the rock material presents complex stress-strain relations under stress, and the continuum damage mechanics, which focuses on studying the continuous deterioration of these defects, is the basic theory to solve this problem [10]. In the continuum damage mechanics, rock masses are regarded as a complex [11–15], which is a composite material consisting of the structure phase and damage phase. With effective bearing area of the structure phase as the basis of the definition of the damage variable, the decrease of the effective bearing area is the damage evolution process of materials; namely, the damage variable can be defined as a ratio of the area of the damage phase to the original area of a cross section area. Zhou and

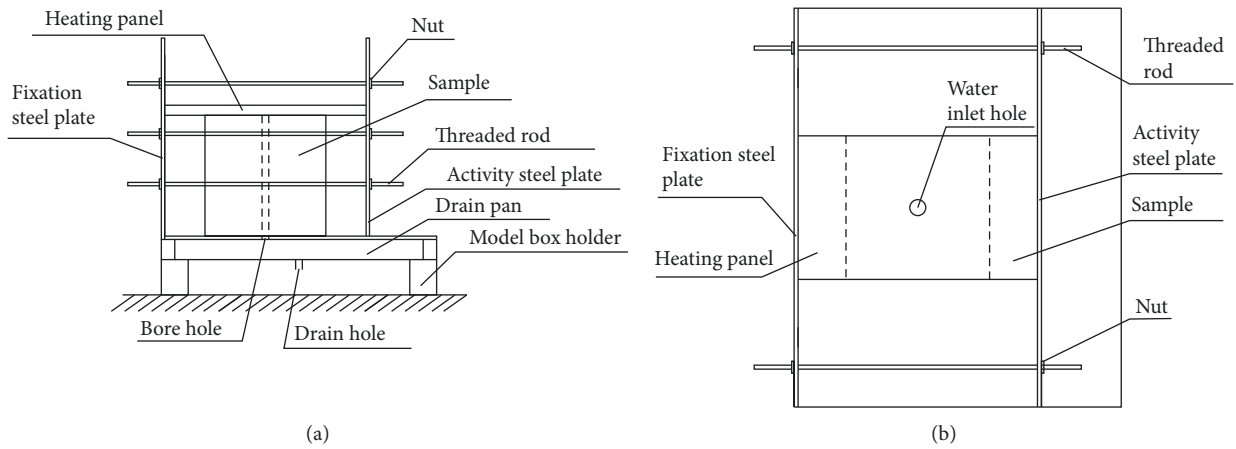

Figure 1: Container used in experiments. (a) Front view. (b) Top view.

Liu [16] obtained the reasonable synthetic mode of stress and strain for a complex theory of geomaterial damage based on the basic concept of continuum mechanics, provided the simplified formulas of the synthetic mode of stress and strain for isotropic damage, and put forward a constitutive model for isotropic damage of geomaterial. Zhou et al. [17] connected the damage variable with cross section areas of the structure phase and damage phase, defined the external force damage power as damage dissipation energy, and introduced it into the soil energy balance equation. Finally, a damage evolution equation is derived based on the energy consumption under the conditions of structural damage.

The damage of rock masses is the process of energy dissipation [18–20], and rock damage after dry-wet cycles also can be regarded as the process of energy dissipation. However, at present, there are few researches about the damage evolution and damage constitutive equation of rock masses under the action of dry-wet cycles. Zhu and Zhou [21] analyzed the forming mechanism of the dissipative structure during the softening process of saturated soft rocks based on the dissipative structure theory. Chen et al. [22] set up damage evolution equation of granite based on the principle of energy dissipation by the uniaxial compression test under multiple dry-wet cycles. According to the irreversible thermodynamics theory, the work done by the external force partly changes into phase transformation damage dissipation energy due to the transformation from the structure phase to the damage phase. There is also a certain energy relationship during the process of dry-wet cycles, and a deeper understanding of the damage characteristics of rock masses under the action dry-wet cycles can be realized by analyzing the energy change law of rock damage. Therefore, a customized model test container and a novel test method are applied to conduct the dry-wet cycle test on mudstone in Chongqing, and the change law of the decay rate under different temperatures and over multiple dry-wet cycles is obtained. According to the experimental results and damage evolution equation based on the energy principle, the damage evolution equation under the coupled action of dry-wet cycles and loads is set up. By comparing the test results from a literature with the proposed model, it shows that the model can properly reflect the damage evolution of mudstone. Finally, the effect of the number of dry-wet cycles on damage is analyzed.

2. Dry-Wet Cycle Test

2.1. Test Process. The experimental materials selected are typical mudstone from the mudstone layers of the Suining Group (its lithostratigraphic unit is marked by J3s), which is located in the Jinfeng district of Chongqing, southwestern China (29°30′46.05″N, 106°18′55.03″E). A total of 9 samples from the same type of mudstone were subjected to nine treatments. To ensure homogeneity, the samples for each treatment were selected from the same mudstone block. And they were cut into similar-sized cubes (180 mm × 180 mm × 180 mm) with an electric saw and drilled through to make to a 15 mm diameter borehole with an electric drill, which was the channel of inlet water and drainage from the centre of the top surface to the bottom surface [23].

The customized testing device, as shown in Figure 1, includes a container, a thermostat-controlled heating panel, and a water supply and drainage unit. The sample is placed in the container, and lateral restraints for the sample are provided by tightening the nuts of the activity steel plate. The heating panel connects in series with a temperature controller, a thermocouple, and a relay, which can control the temperature and maintain a constant temperature.

The dry-wet cycle test is conducted by using the heating plate to heat the sample and by using the top-down drilling hole to maintain water supply and drainage. The test process is as follows: heating for 24 h at 60°C → water exposure for 8 h → heating for 24 h at 60°C → water exposure for 8 h. The period of each cycle is 32 h and so forth.

The temperature is kept constant for drying treatment, involving five subtreatments, at 60°C, 90°C, 105°C, 120°C, and 180°C, respectively. Three dry-wet cycles are conducted at each temperature. Besides, keeping the heating temperature at 60°C, five dry-wet cycles are conducted, that is, 3, 6, 9, 12, and 15, respectively.

After dry-wet cycles, the decay rate of rock was calculated as follows [24]:

Table 1: Effect of constant temperature on rock decay rates (%).

Temperature (°C)	60	90	105	120	180
Number of dry-wet cycles	3	3	3	3	3
Decay rate (%)	0	21.1	25.8	89	89.2
$\alpha(T)$	—	1	1.22	4.22	4.23

Table 2: Effect of the number of dry-wet cycles on rock decay rates (%).

Number of dry-wet cycles	3	6	9	12	15
Temperature (°C)	60	60	60	60	60
Decay rate (%)	0	9.6	16.2	25.6	60.7

$$\mathrm{DR} = \frac{W_{\mathrm{ini}} - W_{\mathrm{rem}}}{W_{\mathrm{ini}}} \times 100\%, \tag{1}$$

where DR = decay rate (%), W_{ini} = initial weight of a sample (grams), and W_{rem} = weight of the largest remaining fragment of a sample (grams).

2.2. Test Results. The effect of constant temperature on the decay rate of rock is shown in Table 1. When the number of dry-wet cycles is equal, the higher temperature the rocks experience, the higher the decay rate.

In Table 1, $\alpha(T)$ is the temperature influence coefficient; if $T = 90^{\circ}\mathrm{C}$, $\alpha(T) = 1$; then, when $T = 105^{\circ}\mathrm{C}$, $\alpha(T) = 25.8/21.1 = 1.22$. By this analogy, $\alpha(T)$ is obtained in Table 1. The relationship between $\alpha(T)$ and temperatures is fitted by a function as follows:

$$\alpha(T) = 4.23 - \frac{3.23}{1 + e^{0.22(T-111.98)}}. \tag{2}$$

The effect of the number of dry-wet cycles on the decay rate is shown in Table 2. When the heating temperature is equal, the decay rate increases with the increase of the number of dry-wet cycles. If the number of dry-wet cycles continuously increases, the decay rate will increase to over 90% until the sample is completely broken.

The relationship between the decay rate and the number of dry-wet cycles in Table 2 is fitted by a function as follows:

$$\mathrm{DR}_{\mathrm{n}} = \frac{90}{1 + e^{-0.3(n-13.7)}}. \tag{3}$$

3. Damage Evolution Equation of Dry-Wet Cycles

3.1. Framework of Damage Evolution Equation. The whole evolution process during dry-wet cycles has inseparable connection with its surroundings, including energy, materials, and information exchange. During dry-wet cycles, the complex mechanism of the action between water and rock is stored in the whole system in the form of energy, which embodies the communication between rock and its surroundings [21]. The research on the law of energy transformation in the process of rock damage is helpful for getting a deeper understanding of the damage of rock masses under the action of dry-wet cycles.

The area of the representative volume element of a rock unit is A, and the density is ρ. The rock unit is composed of the structure phase element and damage phase element. Under a certain stress state, the area of the structure phase element is A_{n} and that of the damage phase element is A_{d}. During the process of dry-wet cycles, the damage of the structure phase leads to the release of elastic energy. When the structure phase element changes into the damage phase element, the strain increment produced by the structure phase is $d\varepsilon_{\mathrm{n}}$ and stress is σ_{n}.

There is a certain relationship between the decay rate (DR) defined in this paper and the damage variable (D). Taking the unit thickness of the rock element, according to the classical continuum damage mechanics, the damage variable is defined as

$$D = \frac{A_{\mathrm{d}}}{A} = 1 - \frac{A_{\mathrm{n}}}{A} = 1 - \frac{A_{\mathrm{n}}\rho}{A\rho} = 1 - \frac{M_{\mathrm{rem}}}{M_{\mathrm{ini}}} = \mathrm{DR}. \tag{4}$$

Therefore, (3) can be expressed as

$$D_{\mathrm{n}} = \frac{90}{1 + e^{-0.3(n-13.7)}}. \tag{5}$$

Equation (5) is the effect of the number of dry-wet cycles on the decay rate at a certain temperature. Introducing the temperature influence coefficient $\alpha(T)$ into (5) can lead to the result of

$$D_{\mathrm{N}} = \alpha(T) D_{\mathrm{n}}. \tag{6}$$

The damage increment based on the energy principle is as follows [17]:

$$dD = \frac{1}{2\Omega}(1 - D)\sigma_{\mathrm{n}} d\varepsilon_{\mathrm{n}}. \tag{7}$$

The combined action between dry-wet cycles and loads accelerates the total damage and shows obvious nonlinear characteristics. Dry-wet cycles can lead to local damage inside rock masses, but the slippage and dislocation between rock grains under the action of loads can limit the action of pore water in the rock masses to some extent, showing that the total damage will weaken under the coupling effect of dry-wet cycles and loads. Therefore, total damage increment under the coupling effect of dry-wet cycles and loads can be expressed as [25]

$$dD_{\mathrm{m}} = dD + dD_{\mathrm{N}} - dD dD_{\mathrm{N}}, \tag{8}$$

where $dD dD_{\mathrm{N}}$ is the coupling phase.

Substituting (6) into (8) leads to the result of

$$dD_{\mathrm{m}} = dD + d\left[\alpha(T) D_{\mathrm{n}}\right] - dD d\left[\alpha(T) D_{\mathrm{n}}\right]. \tag{9}$$

That is,

$$dD_{\mathrm{m}} = dD + d\left[\alpha(T) D_{\mathrm{n}}\right](1 - dD). \tag{10}$$

That is,

$$dD_{\mathrm{m}} = dD + \left[\frac{\partial \alpha(T)}{\partial T} D_{\mathrm{n}} + \frac{\partial D_{\mathrm{n}}}{\partial n}\alpha(T)\right](1 - dD). \tag{11}$$

Introducing (2), (5), and (7) into (11) leads to

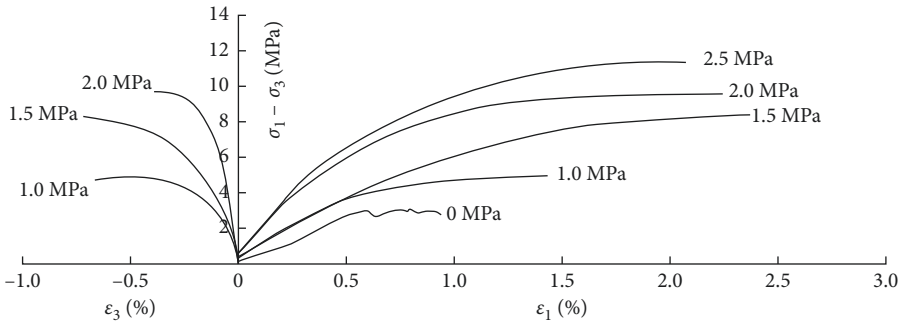

Figure 2: Complete stress-strain curve under different confining pressures [26].

$$dD_{\mathrm{m}} = \frac{1}{2\Omega}(1-D)\sigma_{\mathrm{n}}d\varepsilon_{\mathrm{n}} + \left\{\frac{64.8e^{0.22(T-111.98)}}{\left[1+e^{0.22(T-111.98)}\right]^2\left[1+e^{-0.3(n-13.7)}\right]}dT + \frac{27e^{-0.3(n-13.7)}\left[1+4.23e^{0.22(T-111.98)}\right]}{\left[1+e^{-0.3(n-13.7)}\right]^2\left[1+e^{0.22(T-111.98)}\right]}dn\right\} \times \left[1-\frac{1}{2\Omega}(1-D)\sigma_{\mathrm{n}}d\varepsilon_{\mathrm{n}}\right]. \quad (12)$$

Equation (12) shows that the total damage under the coupling effect of dry-wet cycles and loads changes along with the temperature, the number of dry-wet cycles, and the strain, reflecting the mutually coupled and effected characteristics of the temperature, the number of dry-wet cycles, and the strain to the damage expansion of materials and properly revealing the damage mechanics and damage extension law during dry-wet cycles.

3.2. Constitutive Relation of the Structure Phase. The structure phase is characterized by the elastic state and can be described with the linear elastic model, which is the general Hooke's law. There are principal stresses σ_1, σ_2, and σ_3 in the principal stress space, which satisfy the relationship of $\sigma_1 \geq \sigma_2 \geq \sigma_3$, and the stress increment can be expressed as

$$\begin{aligned} d\sigma_1 &= \alpha_1 d\varepsilon_1 + \alpha_2(d\varepsilon_2 + d\varepsilon_3), \\ d\sigma_2 &= \alpha_1 d\varepsilon_2 + \alpha_2(d\varepsilon_3 + d\varepsilon_1), \\ d\sigma_3 &= \alpha_1 d\varepsilon_3 + \alpha_2(d\varepsilon_1 + d\varepsilon_2), \end{aligned} \quad (13)$$

where $\alpha_1 = K + 4G/3$ and $\alpha_2 = K - 2G/3$, in which K is the bulk modulus and G is the shear modulus.

3.3. Constitutive Relation of the Damage Phase. The damage phase possesses the elastic-plastic energy dissipation mechanism, and the elastic-plastic model can be used to describe its stress-strain relationship. In most cases, the relationship between the residual strength and confining pressure is linear, which can be described by the Mohr–Coulomb condition. Applying the difference between the total strain increment and plastic strain increment to represent the elastic strain increment can obtain

$$\begin{aligned} d\sigma_1 &= \alpha_1 d\varepsilon_1 + \alpha_2(d\varepsilon_2 + d\varepsilon_3) - d\lambda\left(\alpha_1 - \alpha_2 N_\varphi\right), \\ d\sigma_2 &= \alpha_1 d\varepsilon_2 + \alpha_2(d\varepsilon_3 + d\varepsilon_1) - d\lambda\alpha_2\left(1 - N_\varphi\right), \\ d\sigma_3 &= \alpha_1 d\varepsilon_3 + \alpha_2(d\varepsilon_1 + d\varepsilon_2) - d\lambda\left(\alpha_2 - \alpha_1 N_\varphi\right), \end{aligned} \quad (14)$$

where $d\lambda$ is a nonnegative proportion coefficient and $N_\varphi = (1+\sin\varphi)/(1-\sin\varphi)$.

4. Numerical Implementation of the Coupled Model

By using the damage constitutive calculation program developed by FLAC^{3D}, simulations of triaxial compression tests are performed, and the numerical results have been compared with the experimental results in a published literature [26]. The test process in the published article is introduced as follows.

Mudstone with relatively good integrity and uniformity is chosen as the research object. The average density of mudstone is 2.14 g/cm^3, the natural compressive strength with a small variation range is from 2.948 MPa to 3.108 MPa, and the moisture content is 5.1%~7.68%. Mudstone is processed into cylinders with 75 mm diameter and 150 mm height. The test scheme is as follows:

(1) Based on the buried depth and in situ stresses of mudstone, confining pressures of the triaxial compression test are 0 MPa, 1 MPa, 1.5 MPa, 2.0 MPa, and 2.5 MPa, respectively.

(2) Keep confining pressures constant throughout the test and apply displacement control with a rate of 0.5 mm/min to control the test until the sample is broken.

(3) Record the whole stress-strain curves under different confining pressures in real time.

The complete stress-strain curve is shown in Figure 2.

4.1. Parameter Determination of the Structure Phase. When ignoring the bearing capacity of damage parts such as microdefects, the intact rock shows an elastic damage energy dissipation mechanism and reflects its elastic state before damage. In the initial state, the material is all composed of the structure phase; in this case, the elastic modulus and Poisson's ratio of the structure phase can be considered approximately as the elastic parameters of the intact rock in the initial state.

Table 3: Bulk modulus and shear modulus under different confining pressures.

Confining pressure (MPa)	0	1	1.5	2	2.5
Elastic modulus E (GPa)	0.48	0.89	0.91	1.38	1.59
Poisson's ratio	0.3	0.3	0.3	0.3	0.3
Bulk modulus K (GPa)	0.40	0.74	0.76	1.15	1.33
Shear modulus G (GPa)	0.18	0.34	0.35	0.53	0.61

Table 4: Dissipation energy under different confining pressures.

Confining pressure (MPa)	0	1	1.5	2	2.5
Dissipation energy (MJ/m^3)	0.018316	0.053002	0.157756	0.200708	0.218957

According to the published article [26], the relationship between the elastic modulus and confining pressures is shown in Table 3. Based on (15), the bulk modulus and shear modulus under different confining pressures can be calculated, as shown in Table 3:

$$K = \frac{E}{3(1-2\mu)},$$
$$G = \frac{E}{2(1+\mu)}. \tag{15}$$

In the process of axial compression, the energy absorbed by the rock material is the work done by the tester to the sample. When the sample deforms under the effect of confining pressures, the work is also done by confining pressures to the sample. In the conventional triaxial compression experiment, the work is done by the sample in the form of circumferential expansion to the hydraulic oil in the triaxial pressure cylinder, so the actual energy absorbed by rock materials is less than the work done by the tester to the sample in the process of axial compression. Therefore, the actual absorbed energy in the test is

$$K = \int \sigma_1 \, d\varepsilon_1 + 2 \int \sigma_3 \, d\varepsilon_3, \tag{16}$$

where the unit of K is MJ/m^3, which is equivalent to the unit of stress MPa, and ε_1 and ε_3 are the axial strain and circumferential strain, respectively. The circumferential strain is negative, and according to Poisson's ratio effect, it obtains

$$\mu = -\frac{\varepsilon_3}{\varepsilon_1}. \tag{17}$$

According to Figure 2, the relationship between the dissipation energy and the confining pressure can be calculated based on (16), as shown in Table 4.

4.2. Parameter Determination of the Damage Phase. After the complete damage of the structure phase, the rock material turns into a deformation stage of residual strength, and the damage phase bears all the bearing capacity. The damage phase of mudstone shows an elastic-plastic energy dissipation mechanism, and the stress-stain relationship of the damage phase can be described by the elastic-plastic model. The Mohr–Coulomb criterion can be applied to describe the linear relationship between residual strength and confining pressure. The damage phase reflects the stress-strain relationship of the residual strength, so the cohesion and internal friction angle of the damage phase can be obtained by using the regression analysis of experimental data of the residual strength. The elastic modulus and Poisson's ratio of the damage phase can be obtained approximately by using the parameters of class VI surrounding rock.

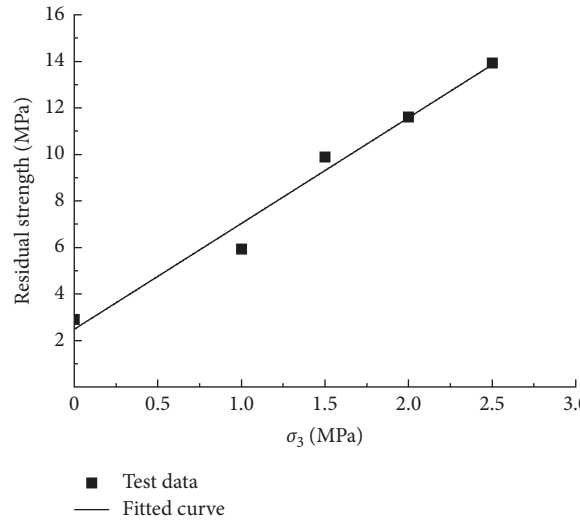

Figure 3: Residual strength under different confining pressures.

The residual strength under different confining pressures based on the experimental results is shown in Figure 3. Because there is no stress decrease to determine the peak strength in Figure 2, the approximate constant stress with the increase of strain is defined as the maximum stress σ_1. The test results show that the residual strength is linearly related to the confining pressure. According to the Mohr–Coulomb criterion, the maximum principal stress of materials can be expressed as $\sigma_1 = \sigma_3 N + \sigma_c$, in which N and σ_c are

$$N = \frac{(1+\sin\phi)}{(1-\sin\phi)} = \tan^2\left(45^\circ + \frac{\phi}{2}\right),$$
$$\sigma_c = \frac{2C\cos\phi}{(1-\sin\phi)}. \tag{18}$$

According to the test results in Figure 3, the fitting equation is $\sigma_1 = 4.5493\sigma_3 + 2.4794$. Based on (18), the strength parameter of the damage phase is $C = 0.581$ MPa and $\varphi = 39.76^\circ$. Assume that the elastic parameters of the damage

Table 5: Material properties of the model.

	Bulk modulus K (GPa)	Shear modulus G (GPa)	Cohesion (MPa)	Internal friction angle (°)	Dissipation energy (MJ/m^3)
Structure phase	Table 3		—	—	Table 4
Damage phase	0.17	0.04	0.581	39.76	—

phase are approximately equal to those of class VI surrounding rock; namely, the bulk modulus is $K_n = 0.17$ GPa and the shear modulus is $G_n = 0.04$ GPa.

All the parameters of the model are listed in Table 5.

4.3. Numerical Simulations for Triaxial Tests. The model dimension is in agreement with that of the published article [26], in which the sample is a cylinder with 75 mm diameter and 150 mm height. The model is divided into 1024 units, as shown in Figure 4. Vertical constraints are imposed at the bottom of the model, and a velocity of 0.5 mm/min is imposed on the top.

By introducing the parameters in Table 5 to the damage constitutive calculation program developed by the FLAC^{3D}, simulations of triaxial compression tests are performed, and the numerical results are compared with experimental results in the published article [26]. The confining pressures σ_3 are 0 MPa, 1 MPa, 1.5 MPa, 2 MPa, and 2.5 MPa, respectively. Because the dry-wet cycle test is not involved in the article [26], the temperature $T = 25$°C and the number of dry-wet cycles $n = 0$ are chosen as the parameters in the numerical simulation. The test results and numerical results under different confining pressures are shown in Figure 5. In the whole simulation process, there is no decrease of stress, which is consistent with the test results. With the increase of confining pressure, the load the damage phase bears increases gradually under the action of confining pressures; thus, there is no obvious decrease of the ultimate bearing capacity after the structure phase element breaks and transforms into the damage phase element, which shows a state of strain hardening, and the residual strength is the peak strength. Therefore, the damage model proposed in this paper can better simulate the characteristics of mudstone materials.

4.4. Effect of the Number of Dry-Wet Cycles. In the dry-wet cycle test, with the increase of the number of dry-wet cycles, the decay rate of mudstone increases, but the elastic modulus, cohesion, and internal friction angle decrease. As shown in Tables 6 and 7, the elastic modulus, cohesion, and internal friction angle under different dry-wet cycles at 105°C are obtained based on [27, 28] and parameters in this paper.

The stress-strain curves and the damage variables with different numbers of dry-wet cycles are shown in Figures 6 and 7. With the increase of the number of dry-wet cycles, the peak deviatoric stress decreases, and the damage develops quickly and early. With the increase of confining pressures, the variation of the peak deviatoric stress and the damage development increases.

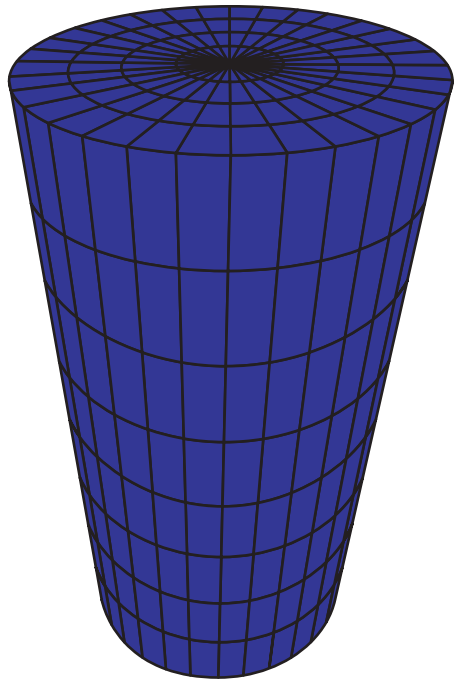

Figure 4: Numerical model.

5. Conclusion

According to the experimental results of dry-wet cycles and the damage evolution equation under the conditions of structural damage energy dissipation, the damage evolution equation under the coupled action of dry-wet cycles and loads is set up. The numerical results are compared with the test results in a published article, which proves the accuracy and validity of the model. The main conclusions can be drawn as follows:

(1) According to the complex damage theory of geotechnical materials, rock masses can be considered as a composite material constituting the structure phase and damage phase. Damage occurs after the elastic deformation energy stored in the internal structure element increases and becomes higher than the critical value. With the continual expansion of the damage phase, the strain energy density dissipated by the material unit increases until the element is completely broken.

(2) According to the effects of temperatures and the number of dry-wet cycles on decay rate, combined with the damage evolution equation based on the energy principle, the damage evolution equation under the coupled action of dry-wet cycles and loads

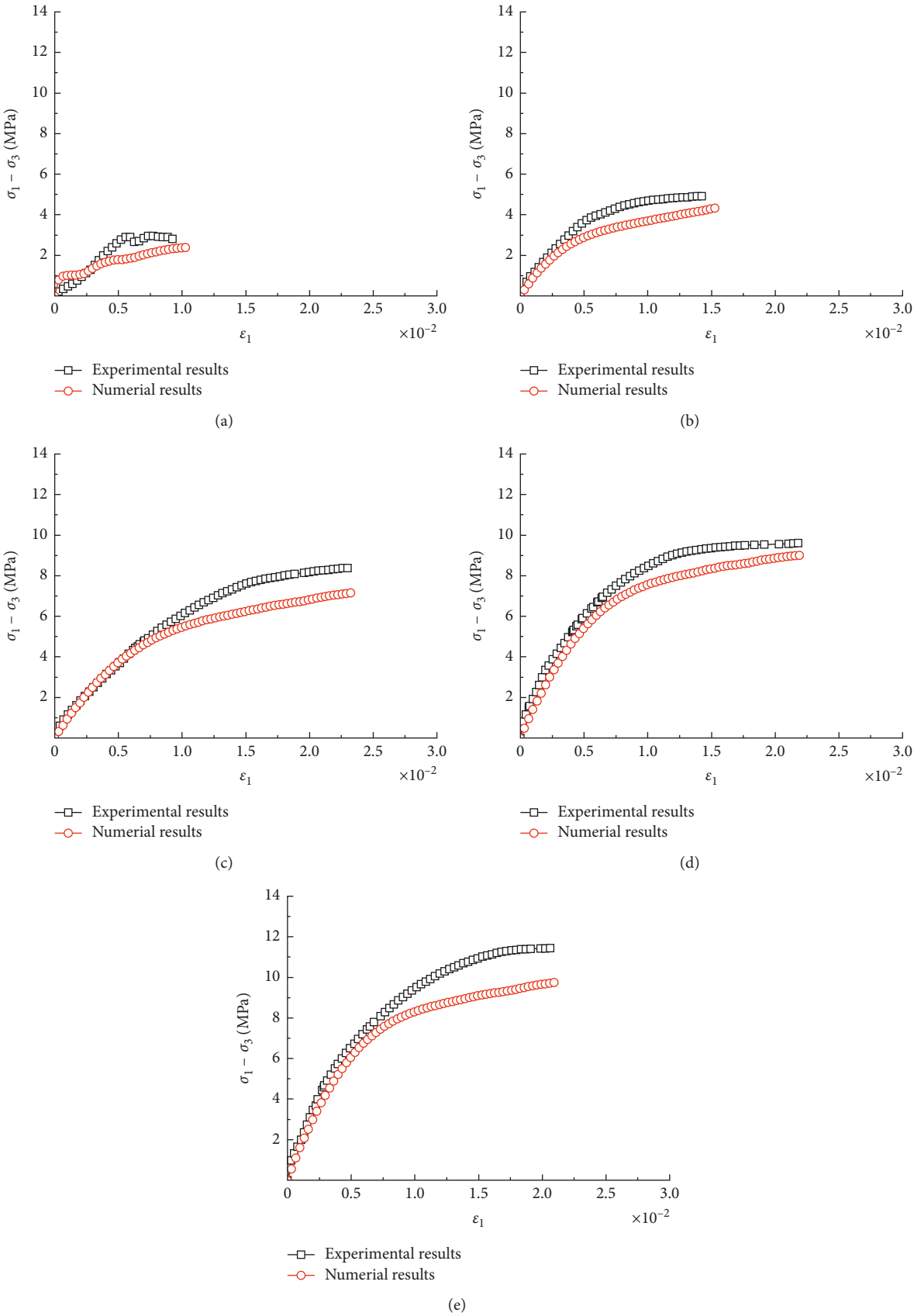

Figure 5: Numerical results and experimental results under different confining pressures: (a) $\sigma_3 = 0$ MPa, (b) $\sigma_3 = 1$ MPa, (c) $\sigma_3 = 1.5$ MPa, (d) $\sigma_3 = 2$ MPa, and (e) $\sigma_3 = 2.5$ MPa.

Table 6: Strength parameters under different dry-wet cycles at 105°C.

Number of dry-wet cycles	3	6	9	12	15
Cohesion (MPa)	0.273	0.168	0.157	0.139	0.122
Internal friction angle (°)	28.07	24.06	23.31	22.84	22.65

Table 7: Elastic parameters under different dry-wet cycles at 105°C.

Number of dry-wet cycles		3	6	9	12	15
Confining pressure (0 MPa)	Elastic modulus E (GPa)	0.120	0.112	0.109	0.106	0103
	Poisson's ratio	0.3	0.3	0.3	0.3	0.3
	Bulk modulus K (GPa)	0.100	0.094	0.091	0.088	0.085
	Shear modulus G (GPa)	0.046	0.043	0.042	0.041	0.039
Confining pressure (2 MPa)	Elastic modulus E (GPa)	0.345	0.323	0.313	0.304	0.295
	Poisson's ratio	0.3	0.3	0.3	0.3	0.3
	Bulk modulus K (GPa)	0.288	0.269	0.261	0.253	0.246
	Shear modulus G (GPa)	0.133	0.124	0.120	0.117	0.113

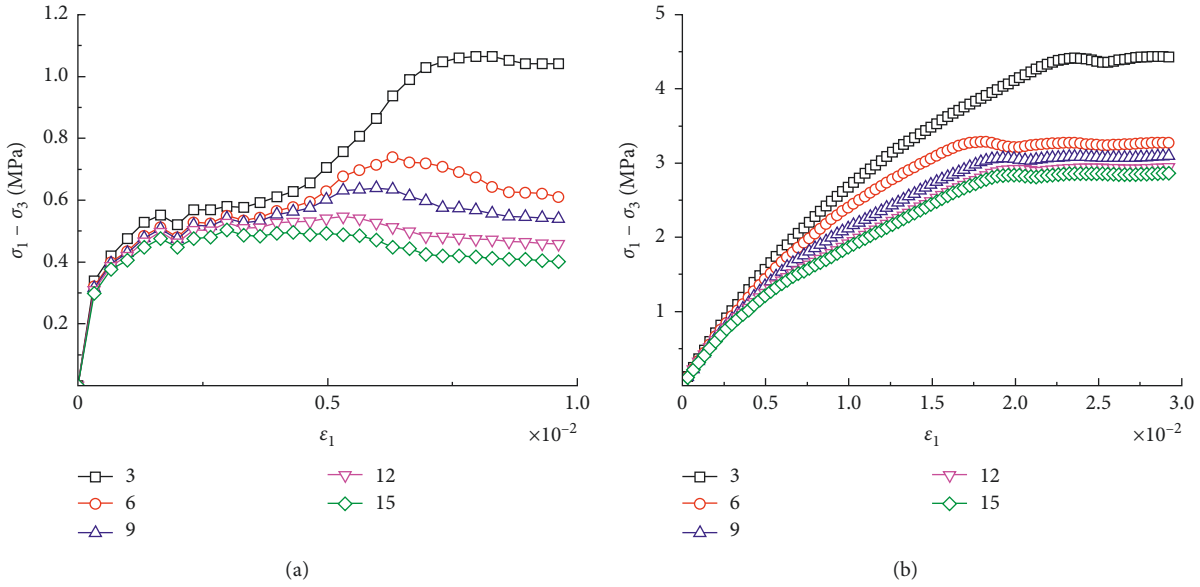

Figure 6: Stress-strain curve under different dry-wet cycles: (a) $\sigma_3 = 0$ MPa and (b) $\sigma_3 = 2$ MPa.

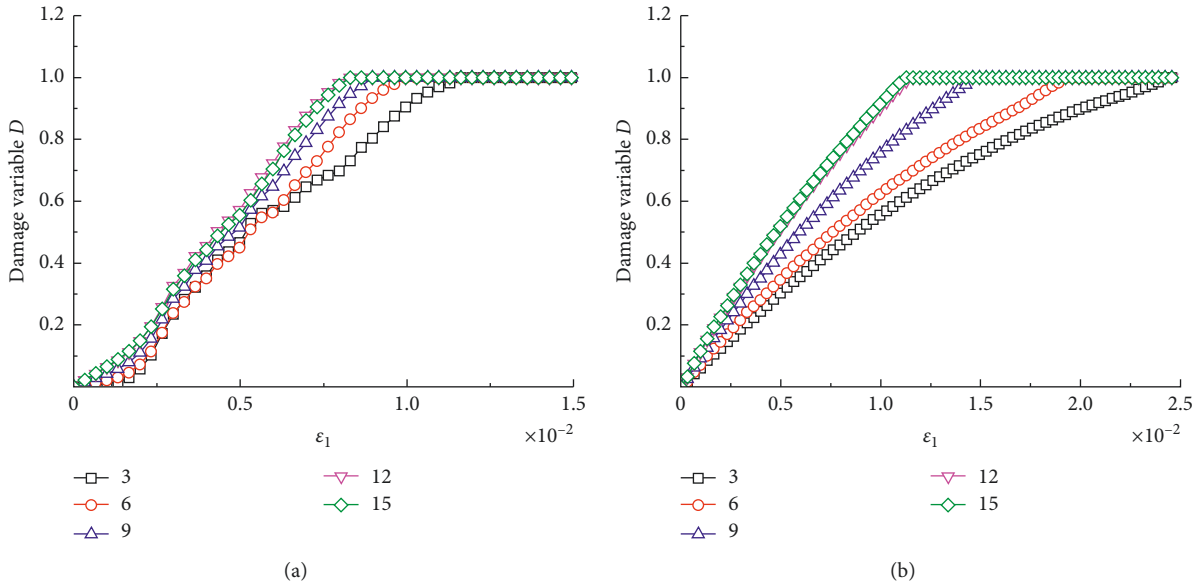

Figure 7: Damage variable under different dry-wet cycles: (a) $\sigma_3 = 0$ MPa and (b) $\sigma_3 = 2$ MPa.

is set up through analyzing the energy of classical units. Comparison of the proposed model with test results in a literature identifies the rationality of the established model.

(3) In this model, the structure phase shows as an elastic state, and the damage phase shows as an elastic-plastic state; therefore, the linear elastic model and the Mohr–Coulomb model are used to study the stress-strain relationship of the structure phase and the damage phase, respectively. Using the damage constitutive calculation program developed by the FLAC^{3D}, simulations of triaxial compression tests are performed, and the effect of the number of dry-wet cycles on damage is analyzed. The results represent that the model can properly reflect the damage evolution of mudstone.

Conflicts of Interest

The authors declare that there are no conflicts of interest.

Acknowledgments

The authors gratefully acknowledge the financial support from the Chongqing Research Program of Basic Research and Frontier Technology (nos. cstc2015jcyjBX0073 and cstc2015jcyjA30007) and the Science and Technology Project of Land Resources and Real Estate Management Bureau of Chongqing Government (KJ-2018016).

References

[1] W. C. Wang, M. M. Wang, and X. L. Liu, "Study on mechanical features of Brazilian splitting fatigue tests of salt rock," *Advances in Civil Engineering*, vol. 2016, Article ID 5436240, 10 pages, 2016.

[2] Y. Cantón, A. Solé-Benet, I. Queralt, and R Pini, "Weathering of a gypsum-calcareous mudstone under semi-arid environment at Tabernas, SE Spain: laboratory and field-based experimental approaches," *CATENA*, vol. 44, no. 2, pp. 111–132, 2001.

[3] Y. C. Guo, Q. Xie, and J. Q. Wen, "Effect of the alternation of heat and water on the slaking phenomenon of redbeds," *Hydrogeology & Engineering Geology*, vol. 39, no. 5, pp. 69–73, 2012.

[4] J. Qi, W. Sui, Y. Liu, and D. Zhang, "Slaking process and mechanisms under static wetting and drying cycles slaking tests in a red strata mudstone," *Geotechnical and Geological Engineering*, vol. 33, no. 4, pp. 959–972, 2015.

[5] Z. Wen, X. Wang, L. Chen, G. Lin, and H. Zhang, "Size effect on acoustic emission characteristics of coal-rock damage evolution," *Advances in Materials Science and Engineering*, vol. 2017, Article ID 3472485, 8 pages, 2017.

[6] J. C. Zhang, W. Y. Xu, H. L. Wang, R. B. Wang, Q. X. Meng, and S. W. Du, "A coupled elastoplastic damage model for brittle rocks and its application in modelling underground excavation," *International Journal of Rock Mechanics and Mining Sciences*, vol. 84, pp. 130–141, 2016.

[7] C. Wei, W. Zhu, S. Chen, and P. G. Ranjith, "A coupled thermal–hydrological–mechanical damage model and its numerical simulations of damage evolution in apse," *Materials*, vol. 9, no. 11, pp. 841–859, 2016.

[8] L. Chen, J. F. Liu, C. P. Wang, J. Liu, R. Su, and J. Wang, "Characterization of damage evolution in granite under compressive stress condition and its effect on permeability," *International Journal of Rock Mechanics and Mining Sciences*, vol. 71, pp. 340–349, 2014.

[9] X. Xu, B. Liu, S. Li, J. Song, M. Li, and J. Mei, "The electrical resistivity and acoustic emission response law and damage evolution of limestone in Brazilian split test," *Advances in Materials Science and Engineering*, vol. 2016, Article ID 8052972, 8 pages, 2016.

[10] H. Z. Li, H. J. Liao, and Q. Sheng, "Study on statistical damage constitutive model of soft rock based on unified strength theory," *Chinese Journal of Rock Mechanics and Engineering*, vol. 25, no. 7, pp. 1331–1336, 2006.

[11] C. S. Desai and Y. Ma, "Modelling of joints and interfaces using the disturbed-state concept," *International Journal for Numerical and Analytical Methods in Geomechanics*, vol. 16, no. 9, pp. 623–653, 1992.

[12] C. S. Desai, C. Shao, and I. J. Park, "Disturbed state modeling of cyclic behavior of soils and interfaces in dynamic soils-structure," in *Proceedings of the Ninth International Conference on Computer Methods and Advances in Geomechains*, pp. 31–42, Wuhan, China, November 1997.

[13] C. S. Desai, *Mechanics of Materials and Interfaces: The Disturbed State Concept*, CRC Press, Boca Raton, FL, USA, 2001.

[14] Z. J. Shen, "An elasto-plastic damage model for cemented clays," *Chinese Journal of Geotechnical Engineering*, vol. 15, no. 3, pp. 21–28, 1993.

[15] Z. J. Shen, "The mathematical model of soil structure," *Chinese Journal of Geotechnical Engineering*, vol. 18, no. 1, pp. 95–97, 1996, in Chinese.

[16] J. T. Zhou and Y. X. Liu, "Constitutive model for isotropic damage of geomaterial," *Chinese Journal of Geotechnical Engineering*, vol. 29, no. 11, pp. 1636–1641, 2007.

[17] J. W. Zhou, Y. X. Liu, and Z. Y. Li, "Damage evolution of structured soil based on energy method," *Chinese Journal of Geotechnical Engineering*, vol. 35, no. 9, pp. 1689–1695, 2013.

[18] H. H. Cheng and M. B. Dusseault, "A continuum damage mechanics model for geomaterials," *International Journal of Rock Mechanics and Mining Sciences*, vol. 41, no. 1, pp. 120–126, 2004.

[19] H. P. Xie, Y. Ju, and L. Y. Li, "Criteria for strength and structural failure of rocks based on energy dissipation and energy release principles," *Chinese Journal of Rock Mechanics and Engineering*, vol. 24, no. 17, pp. 3003–3010, 2005.

[20] P. Wang, J. Xu, X. Fang, and P. Wang, "Energy dissipation and damage evolution analyses for the dynamic compression failure process of red-sandstone after freeze-thaw cycles," *Engineering Geology*, vol. 221, pp. 104–113, 2017.

[21] F. X. Zhu and C. Y. Zhou, "Forming mechanism of dissipative structure in the softening process of saturated soft rocks," *Earth Science—Journal of China University of Geosciences*, vol. 34, no. 3, pp. 525–532, 2009.

[22] X. X. Chen, H. L. Fu, and Z. Qin, "Energy analysis of the evolution of open-pit slope rock damage under the effect of wetting and drying circulation," *Science Technology and Engineering*, vol. 16, no. 20, pp. 247–252, 2016.

[23] M. Hu, Y. Liu, J. Ren, Y. Zhang, and R. Wu, "Temperature-induced deterioration mechanisms in mudstone during dry–wet cycles," *Geotechnical and Geological Engineering*, vol. 35, no. 6, pp. 2965–2976, 2017.

[24] K. Unrug, "Weatherability test of rocks for underground mines," in *Proceedings of the 16th International Conference on Ground Control in Mining*, pp. 259–266, Morgantown, WV, USA, 1997.

[25] H. M. Zhang and G. S. Yang, "Damage mechanical characteristics of rock under freeze-thaw and load coupling," *Engineering Mechanics*, vol. 28, no. 5, pp. 161–165, 2011.

[26] T. L. Han, Y. S. Chen, T. Xie, Z. Yu, and M. M. He, "Experimental study on mechanics characteristics and energy properties of mudstone," *Journal of Water Resources and Architectural Engineering*, vol. 10, no. 3, pp. 116–120, 2012.

[27] X. Q. Liu, S. L. Zhou, M. F. Shang, and Y. Li, "Analysis on mechanical properties of rock based on water-rock interaction," *Journal of Chongqing Jiaotong University*, vol. 31, no. 2, pp. 268–273, 2012.

[28] S. L. Zhou, X. Q. Liu, M. F. Shang, and Y. Li, "Time-varying stability analysis of mudstone reservoir bank based on water-rock interaction," *Rock and Soil Mechanics*, vol. 33, no. 7, pp. 1933–1939, 2012.